



How do temperature, humidity, and air saturation state affect the COVID-19 transmission risk?

Ning Mao¹ · Dingkun Zhang² · Yupei Li¹ · Ying Li³ · Jin Li³ · Li Zhao⁴ · Qingqin Wang⁴ · Zhu Cheng³ · Yin Zhang³ · Enshen Long^{1,3}

Received: 6 April 2022 / Accepted: 27 June 2022 / Published online: 11 August 2022
© The Author(s), under exclusive licence to Springer-Verlag GmbH Germany, part of Springer Nature 2022

Abstract

Environmental parameters have a significant impact on the spread of respiratory viral diseases (temperature (T), relative humidity (RH), and air saturation state). T and RH are strongly correlated with viral inactivation in the air, whereas supersaturated air can promote droplet deposition in the respiratory tract. This study introduces a new concept, the dynamic virus deposition ratio (α), that reflects the dynamic changes in viral inactivation and droplet deposition under varying ambient environments. A non-steady-state-modified Wells–Riley model is established to predict the infection risk of shared air space and highlight the high-risk environmental conditions. Findings reveal that a rise in T would significantly reduce the transmission of COVID-19 in the cold season, while the effect is not significant in the hot season. The infection risk under low-T and high-RH conditions, such as the frozen seafood market, is substantially underestimated, which should be taken seriously. The study encourages selected containment measures against high-risk environmental conditions and cross-discipline management in the public health crisis based on meteorology, government, and medical research.

Keywords Temperature · Relative humidity · Air saturation state · COVID-19 · Respiratory tract deposition · Transmission risk model

Introduction

The novel coronavirus disease 2019 (COVID-19) has stimulated unprecedented public health concerns (Azman and Luquero 2020; Liu et al. 2020b; Morawska et al. 2020).

Responsible Editor: Lotfi Aleya

✉ Enshen Long
longes2@scu.edu.cn

Ning Mao
cdmaoning@qq.com

Dingkun Zhang
zhangdk14@tsinghua.org.cn

Yupei Li
sculyp@163.com

Ying Li
1220884690@qq.com

Jin Li
hvaclijin@163.com

Li Zhao
Zhaolicabr@163.com

Qingqin Wang
wngqq@cabr.com.cn

Zhu Cheng
scchengzhu@126.com

Yin Zhang
cdzhangyin@163.com

- ¹ MOE Key Laboratory of Deep Earth Science and Engineering, Institute of Disaster Management and Reconstruction, Sichuan University, Chengdu, China
- ² Laboratory of Clinical Proteomics and Metabolomics, Institutes for Systems Genetics, West China Hospital, Sichuan University, Chengdu, China
- ³ College of Architecture and Environment, Sichuan University, Chengdu, China
- ⁴ China Academy of Building Research, Beijing, China

Two years have passed since its early outbreak, COVID-19 prevention has destined to be a prolonged battle. It is impracticable for all human active areas to take long-term disinfection and isolation of activities. Therefore, our attention needs to be directed to high-risk areas (Coccia 2021b). Without considering other artificial factors, an urgent need is to identify the exposure scenarios that may promote COVID-19 transmission.

It has been reported that seasonal cyclicality is a ubiquitous feature of acute infectious diseases, which is also commonly observed in respiratory viral diseases, such as SARS and MERS (Killerby et al. 2018; Wang et al. 2020). Therefore, it is reasonable to speculate that environmental and meteorological factors affect the COVID-19 (Xie and Zhu 2020). The analysis of how certain meteorological conditions may have affected the initial spread of COVID-19 at the country, city, or regional level has become an important line of research recently (Li et al. 2022; Rahimi et al. 2021). To control the pandemic, many studies have examined meteorological/weather conditions that might influence the spread of coronaviruses by exploring the association between these factors and the COVID-19 cases over different worldwide locations (see Appendix A: Table A.1).

Some scholars only selected T and RH to analyze the correlation between meteorological parameters and the spread of COVID-19 (absolute humidity and rainfall are also considered as a form of humidity). The preliminary results showed T and RH significantly related to the transmission risk (Haque and Rahman 2020; Mendez-Arriaga 2020; Pani et al. 2020; Prata et al. 2020; Sobral et al. 2020; Tosepu et al. 2020; Wu et al. 2020).

Some scholars not only focused on T and RH but also comprehensively analyzed the other meteorological parameters, such as solar radiation, wind speed, and air pollutant (Diao et al. 2021; Ma et al. 2020; Menebo 2020; Rosario et al. 2020; Runkle et al. 2020; Şahin 2020; Xu et al. 2020a). The solar radiation showed a negligible on the COVID-19 transmission, even in the comparison of high- and low-altitude regions (Song et al. 2022). The cities with low wind speed and high levels of air pollution exceeding safe levels of particulate matter had higher numbers of COVID-19-related cases and deaths (Coccia 2020c, a, 2021a, c, d, 2022b).

In addition, many scholars did their epidemic research from many different angles and combined meteorological parameters (T and RH) with population mobility. The conclusion is obvious that the higher population density and migration scale tends to prolong the spread (Ahmadi et al. 2020; Diao et al. 2021; Lin et al. 2020; Liu et al. 2020a).

In brief, T and RH are not only the main meteorological parameters widely analyzed by scholars but also significantly correlated with the COVID-19 pandemic, even

with the incorporation of additional variables and controls (solar radiation, wind speed, and air pollutant, and population migrated).

However, the association between meteorological parameters and COVID-19 cases also would be affected by local artificial factors, including social, political, and economic (Lai et al. 2020). The results in quantifying environmental effects on transmission risk are limited and equivocal (Briz-Redón and Serrano-Aroca 2020).

Therefore, to reject the effect of other social factors, quantifiable mathematical models of transmission risk are needed (Bin et al. 2018; Borro et al. 2020; Qian et al. 2012; Sharma and Balasubramanian 2020). Wells-Riley model (W-R model) is one of the most popular models for quantitatively assessing the infection risk of airborne diseases (Keene 1955; Riley et al. 1978; Vuorinen et al. 2020; Wagner et al. 2009; Zhang et al. 2020). Understandably, the W-R model has been further improved and extended by many latest studies to include more realistic factors and considerations since the COVID-19 outbreak. For instance, Nordsiek et al. developed an optimization W-R model for computational risk assessment suitable for mono/poly-pathogen aerosols (Nordsiek et al. 2021). Andrews et al. used a modified W-R model to estimate the impact of ventilation on infection probability for inmates sharing a cell with an infector (Urrego et al. 2015). Zhou and Koutsopoulos proposed a modified W-R model for risk analysis in public transportation systems, which integrated with a simulation model of subway operations (Zhou and Koutsopoulos 2021). Zhai et al. and Zhang et al. developed a modified W-R model for integrating the spatial distribution of pathogen concentrations (Guo et al. 2021; Zhai and Li 2021). Fierce et al. tried to develop the quadrature-based model of droplet risk by introducing a dose-response framework, which could reflect the evolution of particles after they are expelled, their deposition in the airways, and the subsequent risk of initial infection (Fierce et al. 2021).

Although the various studies above used different methods for risk analysis of airborne diseases, they collectively treated the shared air space as a close-to-greenhouse environment. The T, RH, and P_v are assumed to be constant. However, the epidemic outbreak in different regions keeps transmitting under varying environmental parameters. It can be seen from Table 1 that those environmental parameters were believed to significantly promote or inhibit the spread of COVID-19. Therefore, a non-steady-state-modified Wells-Riley model of the dynamic change of environmental parameters is required.

This study aims to answer the following questions: How are T, RH, and P_v linked to infection risk? Which exposure scenarios promote or inhibit COVID-19 transmission? The answers to these questions will help local healthcare

Table 1 Control parameters for different exposure scenarios

Environment parameters	Case 1	Case 2	Case 3	Case 4	Case 5	Case 6
Temperature ^a (T, °C)	40	60	20	24	20	5
Relative humidity ^b (RH, %)	90	50	30	60	80	95
Viral inactivation (λ , h ⁻¹)	0.8	0.99	0.4	0.9	0.2	0.15
Saturated vapor pressure (P_v , hPa)	66.37	99.64	7.01	17.9	18.7	8.3
Vapor pressure difference ^c ($ P_v - P_{vo} $, hPa)	4.27	37.5	55.1	44.2	43.4	53.8

^aHigh temperature: T > 30 °C; middle temperature: 10 °C < T < 30 °C; low temperature: T < 30 °C

^bHigher humidity: RH > 80%; middle humidity: 40% < RH < 80%; lower humidity: RH < 30%

^cAbsolute value of the saturated vapor pressure difference between ambient air and respiratory tract air

Respiratory boundary conditions: T = 37 °C, RH = 99%, and P_{vo} = 62.1 hPa

polymakers grade human activity regions according to the COVID-19 transmission risk.

Materials and methods

Sample and data

A thorough understanding of infectious droplets is a primary factor in the study of COVID-19 airborne transmission risks, such as the diameter distribution, SARS-CoV-2 viral load, viral inactivation in the air, and deposition fraction in the respiratory tract. This study summarizes the number distribution of exhaled droplets from different respiratory activities and the viral load in the body fluids of infected persons (see Appendix A: Table A.2 and Table A.3, respectively).

Notably, the viral inactivation in the air and the droplet deposition in the respiratory tract are significantly influenced by ambient environmental factors (T, RH, and P_v) and should be discussed with emphasis (Ishmatov 2020; Longest et al. 2011; Xi et al. 2015; Xie and Zhu 2020).

Viral inactivation characteristics in the air

The significant changes in virus survival balance after being exhaled from the infector lead to differences in the disease infection risk in different environments (Pica and Bouvier 2012; van Doremalen et al. 2020; Wei and Li 2016). Therefore, several scholars have conducted studies on aerosolized viral inactivation under varying T and RH and aerosolized the viruses into a rotating drum, where the aerosols were held at the desired T and RH. Following this, the samples of air from the drum were collected using an impinger (Doremalen et al. 2013; Pyankov et al. 2018; Sattar et al. 1984). This study summarizes viral inactivation characteristic of respiratory disease under varying T and RH, as shown in Appendix A: Figure A.1 and Table A.4

When T was at a specific value (22–25 °C), the viruses were found to survive better at low-RH levels (<33%) and high-RH levels (>85%). The middle-RH level (50–75%)

was found to be the least favorable for the survival of the viruses. And, within the range of certain RH, there was a significant negative correlation between the viral inactivation rate and T (Colas et al. 2014; Harper 1961; Lin and Marr 2020b; Noti et al. 2013). Therefore, the viral inactivation rate in the air (λ) is significantly affected by the ambient T and RH, which further inhibits or promotes the spread of an epidemic in local areas (Mao et al. 2020; Walsh et al. 2020).

Droplet deposition in the respiratory tract

Diameter growth of inhaled droplets in the airways To analyze pulmonary drug delivery, plenty of studies on particle deposition in the airways have been conducted by medical scholars (Austin et al. 2010; Gralton et al. 2011; Knight 2010; Morrow 2010; Nicas et al. 2005; Yeh and Raabe 1976). During inhalation, when the respiratory tract air (T = 37 °C, RH = 99% (Winkler-Heil et al. 2017)) is mixed with the inhaled ambient air (relatively low RH and T), the small particle (<10 μ m) can grow owing to condensation. Therefore, the concept of enhanced condensational growth (ECG effect) was proposed by medical scholars in which a drug aerosol is inhaled in combination with cold-saturated air; this would cause the small particle diameter to increase, thereby promoting lung drug deposition (Deng et al. 2020; Longest and Hindle 2010, 2011; Longest et al. 2011; Tian et al. 2011). The diameter growth factors of inhaled supersaturation droplets in the airways are summarized (Kim et al. 2013; Kreyling 1984; Longest et al. 2011; Sarangapani and Wexler 1996; Xi et al. 2013; Xi et al. 2015) (see Appendix A: Table A.5, and Figure A.2). Understandably, the ECG effect would also increase the deposition risk of infectious droplets.

Droplet deposition fraction in the respiratory tract It is known that viruses can only cause infection when inhaled by susceptible populations and when successfully deposited in the respiratory tract (Akhbarizadeh et al. 2021; Pu et al.

2020). Furthermore, the deposition fraction of infectious droplets is dependent on the aerosol droplet diameter distribution (Asgari et al. 2019; Fröhlich-Nowoisky et al. 2016). Figure 1 summarizes the distribution of exhaled droplets from different respiratory activities and the corresponding deposition fractions in the respiratory tract (ICRP 1994).

Large particles are mainly deposited through inertial impaction, whereas small particles are mainly deposited through molecular diffusion (Fröhlich-Nowoisky et al. 2016). It is noteworthy that supersaturated air can lead to significant growth in inhaled small particle diameter in the airways due to the ECG effect. For example, the total deposition of 0.3- μm particles in the airways may rise from 13% (when supersaturation is not considered) to 90% (under supersaturated conditions). It is evident that the infection risk is set to surge.

Measures of variables

Viral inactivation rate in the air (λ)

The viral inactivation rate in the air (λ) is significantly affected by the ambient T and RH, which further inhibits or promotes the spread of an epidemic in local areas. The value of λ was selected from existing studies on aerosolized viral inactivation under varying T and RH (Appendix A: Table A.4)

Dynamic virus deposition ratio (α)

Considering the dynamic changes in particle size and viral deposition in different ambient environments, our study proposes a new term, the dynamic virus deposition ratio (α) (Eq. (1)), which is defined as the ratio between the viral load deposited in the respiratory tract under varying environments ($Q_{\text{deposition}}$) and the total viral load inhaled by a susceptible population (Q_{total}).

$$\alpha = \frac{Q_{\text{deposition}}}{Q_{\text{total}}} \tag{1}$$

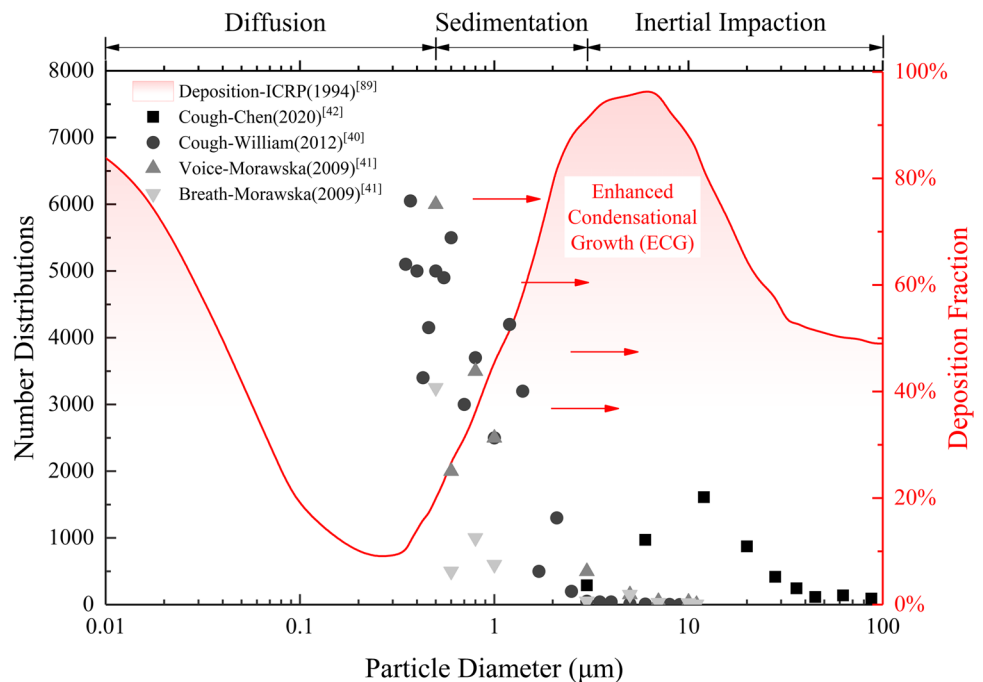
where $Q_{\text{deposition}}$ is the viral load deposited in the respiratory tract under varying ambient environments (RNA copies), and Q_{total} is the total viral load inhaled by a susceptible population (RNA copies).

$$Q_{\text{deposition}} = \sum_{i=1}^n (C'_{V,i} \cdot p \cdot N'_i \cdot V'_i(d) \cdot \omega'_i) \tag{2}$$

$$Q_{\text{total}} = \sum_{i=1}^n (C_V \cdot p \cdot N_i \cdot V_i(d_0)) \tag{3}$$

where $C'_{V,i}$ is the viral concentration of droplets with i diameter after considering the ECG effect on particle size (RNA copies/mL), N'_i is the number of droplets with i diameter after considering the ECG effect on particle size (part. m–3), $V'_i(d)$ is the volume of a single droplet (mL) as a function of the droplet diameter after considering the ECG effect on particle size (d), and ω'_i is the deposition fraction of droplets with i diameter after considering the ECG effect

Fig. 1 Number distribution of exhaled droplets from different respiratory activities and the corresponding deposition fraction in the respiratory tract



on particle size (the values were selected according to the ICRP data (ICRP 1994)).

The supersaturation diameter growth factors for inhaled air with different saturated vapor pressures (d/d_0) can be calculated from the following equation (Xi et al. 2015):

$$\frac{d}{d_0} = 1 + \frac{0.865 \cdot |P_v - P_{v,o}|^{0.293}}{d_i^{1.13}} \quad (4)$$

where P_v is the saturated vapor pressure of the ambient air (hPa), and $P_{v,o}$ is the saturated vapor pressure of air in the respiratory tract ($T = 37^\circ\text{C}$, $\text{RH} = 99\%$, $P_v = 62.1$ hPa).

However, droplet condensation in the airways (ECG effect) changes their particle size (d'_i), which modifies the concentration of viral charges in the droplets ($C'_{v,i}$, copies/mL) due to a higher water fraction. Meanwhile, it should not change the absolute number of viral copies in the droplet. (For example, a 1- μm droplet has the same number of viral charges after condensation, whereas their concentration is reduced owing to a higher liquid volume.) Therefore, the absolute number of viral copies in a droplet with i diameter after considering the ECG effect can only be a dynamic cumulative value (Eq. (5)), not directly calculated by the original volume and concentration (Eq. (2)).

$$Q'_{\text{deposition}} = \sum_{i=1}^n (C'_{\text{cum},i} \cdot \omega'_i) \quad (5)$$

$$\alpha = \frac{\sum_{i=1}^n (C'_{\text{cum},i} \cdot \omega'_i)}{\sum_{i=1}^n (C_v \cdot p \cdot N_i \cdot V_i(d_0))} \quad (6)$$

where $C'_{\text{cum},i}$ is the total viral load of droplets with diameter i after considering the ECG effect on the particle size (RNA copies).

Model and data analysis procedure

Modified Wells-Riley model

Quanta emission A quantum is defined as the dose of airborne droplet nuclei required to cause infection in 63% of susceptible persons. In the original W-R model, the quanta emission rate remains uncertain and highly variable (Gba et al. 2020; Harrichandra et al. 2020). To estimate the spatiotemporal variation in virion concentrations, an Italian scholar, Buonanno, developed a modified W-R model based on a dose-response method to calculate the virion emission rate through a mass balance, which allows consideration of per-particle variation in viral load and the airborne transmission risk between scenarios (Buonanno et al. 2020). In particular, the viral load emitted was expressed in terms of the quanta emission rate (ER).

$$ER_j = C_v \cdot C_i \cdot p \cdot \sum_{\substack{1 \leq i \leq n \\ 1 \leq j \leq m}} (N_{ij} \cdot V_i(d_0)) \quad (7)$$

where ER_j is the quanta emission rate from different respiratory activities (quanta h^{-1}), j indicates the different respiratory activities considered (breath = 1, voice = 2, cough = 3), C_v is the viral concentration in the throat of the asymptomatic infector (RNA copies/mL), C_i is a conversion factor defined as the ratio between one infectious quantum and the infectious dose expressed in viral RNA copies (Li et al. 2010; Watanabe et al. 2010; Yu et al. 2004) (0.01–0.1), p is the breathing rate per person (Marmett et al. 2020) (m^3/s), N_{ij} is the number of droplets with i diameter from j respiratory activities, and $V_i(d_0)$ is the volume of a single droplet (mL) as a function of the droplet diameter (d_0); the droplets are assumed to be standard spheres.

Quanta concentration of the shared air space After being expelled from the infector, the quanta concentration at time t (Gammaitoni and Nucci 1997), $n(t)$, as follows:

$$n(t)_j = \frac{ER_j \cdot I}{(AER + K + \lambda) \cdot V} (1 - e^{-(AER+K+\lambda)t}) \quad (8)$$

where $n(t)_j$ is the quanta concentration from different respiratory activities at time t , I is the number of asymptomatic infectors, AER is the air exchange rate via ventilation (natural ventilation (Alfano et al. 2012, Stabile et al. 2017), 0.2 h^{-1}), K is the particle deposition on surfaces (released from 1.5 m at a speed of $1 \times 10^{-4} \text{ m/s}$ (Chatoutsidou and Lazaridis 2019), 0.24 h^{-1}), λ is the viral inactivation rate of respiratory disease (the values were selected according to Appendix A: Table A.4), V is the volume of the shared air space (m^{-3}), and t is the exposure time (s).

Infection risk under varying environments Thereafter, the dynamic virus deposition ratio, α , is used to correct the breathing rate of the susceptible population, p , and the modified dimensionless inhalation rate, p' , is expected to reflect the dynamic risk due to the ECG effect more accurately.

$$p' = p \cdot \alpha \quad (9)$$

Infection risk ($R_{j,t}$, %) as a function of exposure time (t) of susceptible people.

$$R_{j,t} = 1 - e^{-p' \cdot \int_0^t n(t) dt} \quad (10)$$

In the end, the basic reproductive number (R_0) could be calculated if we multiply the peak of infection risk by the number of all exposed persons during the exposure time (Rothman et al. 2011).

Data analysis procedure

Example case ECG effect is a concept of pulmonary drug delivery in which the drug aerosol is inhaled combination with cold-supersaturated air. The subsequent small particle condensation growth will promote lung drug deposition (Xi et al. 2015). Similarly, the ECG effect would increase the virus deposition risk of airborne diseases.

To illustrate the impact of ECG effect on respiratory particle deposition and Virion exposure, this paper presents the calculation process of dynamic virus deposition ratio, α , in typical cold-saturated conditions (example case: $T = 5\text{ }^\circ\text{C}$, $RH = 95\%$), as shown in Fig. 4.

According to Eq. (4), the droplet diameter would change during inhalation. The smaller the particle size, the bigger the growth factor, and only a small particle ($<10\text{ }\mu\text{m}$) shows significantly grow (see Fig. 2(a)). It is assumed that these droplets are deposited after condensation, and the final droplet distribution ranged from 3 to $100\text{ }\mu\text{m}$. This change is unfortunate to reach the high-risk deposition peak in the airways (see Fig. 2(b)). As a result, the number of deposited particles increased by 3 times (see Fig. 2(c)), and the dynamic virus deposition ratio, α , of this condition could go as high as 51.94% (see Fig. 2(d)). Thus, it is evident that the virion exposure and infection risk increases dramatically (example case: $T = 5\text{ }^\circ\text{C}$, $RH = 95\%$).

Results

Quanta emission rate from different respiratory activities

Figure 3 shows the ER_j (quanta. h^{-1}) trends as a function of time and viral load in the throat (C_v , Log_{10} RNA copies. mL^{-1}) and the quanta-RNA copies correction factor (C_p , 0.01-0.1) from three respiratory activities (breath, voice, cough) and light exercise activity level (p , $1.38\text{ m}^3/\text{h}$). For the sole purpose of simplifying the discussion, zones representative of low (<1 quantum h^{-1}) and high (>1 quantum h^{-1}) quanta emission are separated by the red dotted line indicated (ER_j , 1 quantum h^{-1}).

The trends of the quanta emission rate are similar to that of the viral load of SARS-CoV-2 in a patient’s body fluids, peaking approximately 4 to 6 days after onset and then decreasing over time. In the case involving typical clinical symptoms of the COVID-19 patient (cough condition), the quanta emission rate covers the range of 10^{-4} to 10^5 quanta. h^{-1} , up to 5.55×10^4 quanta. h^{-1} . A high emission in the case of coughing was achieved at 11 days out of 15. Speech is one of the most important communication methods between people (voice condition). The quanta emission rate covering the range of 10^{-5} to 10^4 quanta.

Fig. 2 Calculation process of dynamic virus deposition ratio, α , in typical cold-saturated condition (example case: $T = 5\text{ }^\circ\text{C}$, $RH = 95\%$)

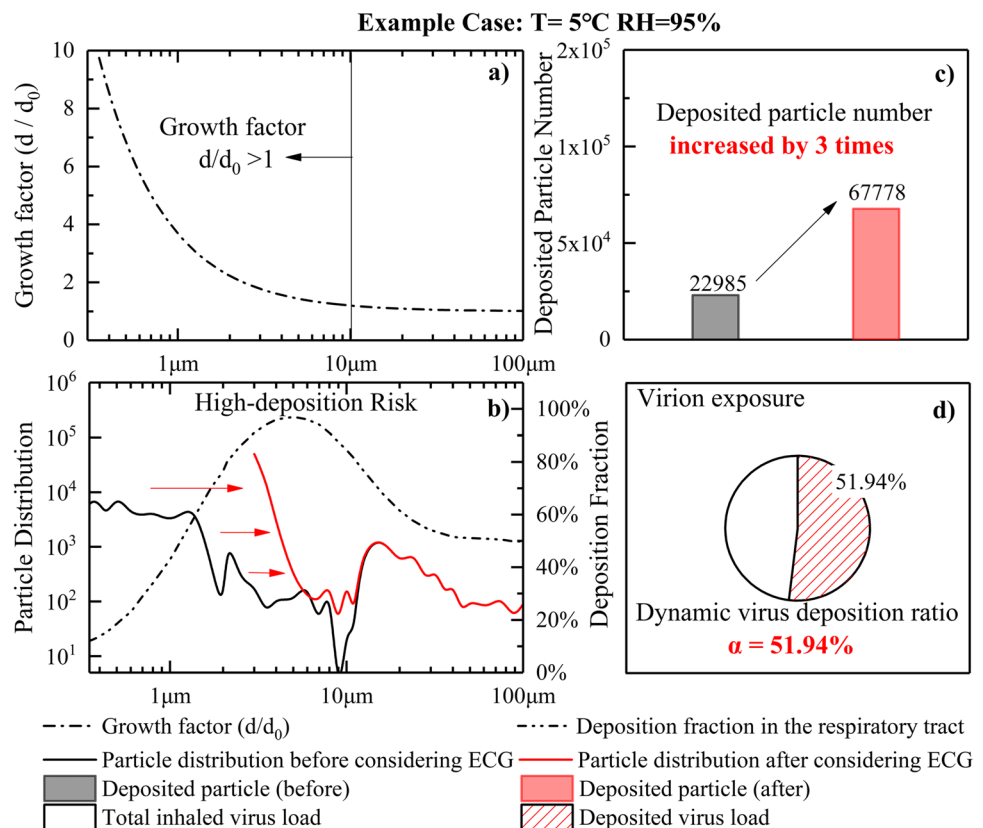


Fig. 3 ER_j (quantum. h^{-1}) trends as a function of the time and the viral concentration in the throat (C_v , Log_{10} RNA copies. mL^{-1}) and quanta-RNA copies correction factor (C_r , 0.01-0.1) for the three respiratory activities (breath, voice, cough). Only the first 15 days of data are calculated after onset. Zones representative of low (<1 quantum h^{-1}) and high (>1 quantum h^{-1}) quanta emission are separated by the red dotted line indicated

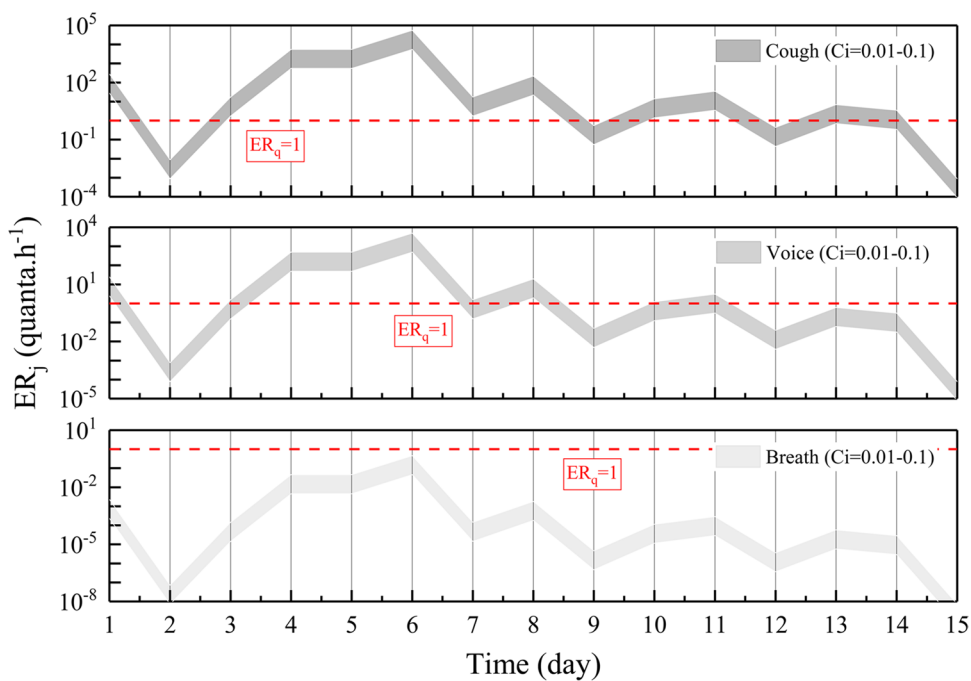
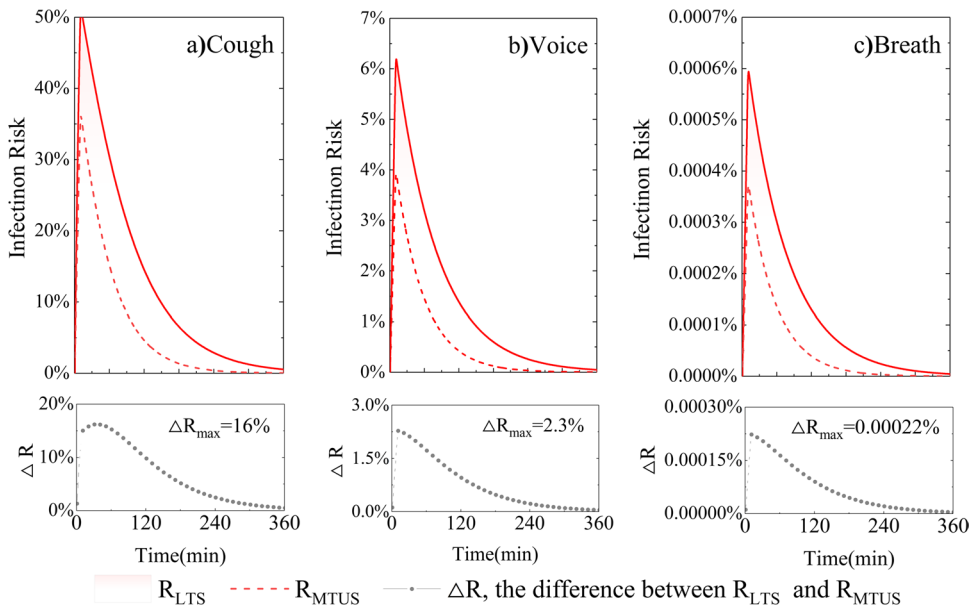


Fig. 4 Infection risk trends as a function of time (an asymptomatic infector remained inside the space for 10 min). The difference (ΔR) between R_{LTS} ($T = 10^\circ\text{C}$, $\text{RH} = 100\%$) and R_{MTUS} ($T = 25^\circ\text{C}$, $\text{RH} = 60\%$) for three respiratory activities (cough, voice, breath) are compared, respectively



h^{-1} is approximately 1/10 of the coughing condition. A high emission in the case of speaking can be achieved only at five days out of 15. It is noteworthy that breathing is a continuous behavior of an asymptomatic person during his/her daily activities (breath condition). Although the quanta emission rate fails to achieve a high emission zone in the breath condition, more viruses might accumulate

over time due to having a higher frequency than cough and voice conditions.

Infection risk for different environments

This section aims to show how the environmental parameters (T , RH , and P_v) are linked to the disease transmission risk in two different microenvironments, low-temperature-saturated condition (low-T: $T = 10^\circ\text{C}$, saturated: $\text{RH} = 100\%$, R_{LTS}) and middle-temperature-unsaturated condition (middle-T:

$T = 25\text{ }^{\circ}\text{C}$, unsaturated: $\text{RH} = 60\%$, R_{MTUS}). The following input data are defined: C_v is 10^8 RNA copies/mL, AER is 0.2 h^{-1} (natural ventilation (Buonanno et al. 2020)), K is 0.24 h^{-1} (Chatoutsidou and Lazaridis 2019), λ is 0.4 h^{-1} and 0.8 h^{-1} respectively for R_{LTS} and R_{MTUS} (according to Appendix A: Table A.4), C_i is 0.02 (Watanabe et al. 2010), V is $8\text{ m} \times 6\text{ m} \times 3.5\text{ m} = 168\text{ m}^3$, and p is $1.38\text{ m}^3 \cdot \text{h}^{-1}$ (light exercise activity level (Adams 1993)). It is assumed that only an asymptomatic infector remained inside the environment for 10 min; the infection risk is simulated for up to 6 h, as shown in Fig. 4.

The trends highlight that the brief stopover of the asymptomatic infector in the microenvironments leads to a peak risk of infection at 10 min. The more intense the respiratory activity, the higher the quanta emission rate. Therefore, the highest disease infection risk was 50% for cough, 6.2% for voice, and 1.2% for breath. In particular, it is known from the literature mentioned above that the viruses are found to survive better in low-temperature air, and the subsequent particle growth of inhaled supersaturated air promotes lung deposition. Therefore, it is understandable that a higher peak infection risk is reached at R_{LTS} ($T = 10\text{ }^{\circ}\text{C}$, $\text{RH} = 100\%$) rather than R_{MTUS} ($T = 25\text{ }^{\circ}\text{C}$, $\text{RH} = 60\%$). Cough, $\Delta R = 15 \pm 3.3\%$, $p < 0.01$; Voice, $\Delta R = 2 \pm 0.5\%$, $p < 0.01$; Breath, $\Delta R = 0.0022 \pm 0.0006\%$, $p < 0.01$.

Typical scenarios studies

The research results in the “Infection risk for different environments” section support the argument that infection risk varies with the environment. Therefore, six typical exposure scenarios from daily life were chosen to analyze the effects of environmental parameters on disease transmission risk. The control parameters for the different exposure scenarios are summarized in Table 1.

First, the exposure scenarios of the shower room (case 1, high- T and high- RH conditions (China 1998)), and the sauna (case 2, high- T and middle- RH conditions (China 1998)) were selected to analyze the infection risk under high temperature. Second, the most common exposure scenario during daily life is selected as a comparison condition (case 4, middle- T and middle- RH conditions (China 2017)). As the flu season approaches, the indoor exposure scenarios during the rainy condition in autumn (case 5, middle- T and high- RH conditions (Nan et al. 2009)) and during heating conditions in winter (case 3, middle- T and low- RH conditions (Yan 2015)) were selected to analyze the infection risk under middle temperature. Finally, based on the conclusions in the “Model and data analysis procedure” section, the infection risk in the scenario (cold and damp) must be taken seriously. Therefore, the extreme typical exposure scenario of the seafood cold store (case 6, low- T and high- RH conditions (China 2010)) is analyzed.

For all the typical exposure scenarios considered in the simulations, the asymptomatic infector remains inside the environment for 5 min, as shown in Fig. 5. The aim is to compare the infection risk during speaking (voice, $j = 2$) in the shared air space. For this reason, the following assumptions for all scenarios are defined: 4 persons are always present; 1 new visitor every 5 min enters; every visitor remains inside for 5 min; thus, 5 persons are simultaneously present. The other input data is consistent with the “Infection risk for different environments” section.

Although the quanta emission rate is consistent in each scenario, viral inactivation in the air (λ) and the deposition fraction in the respiratory tract (ω) are significantly influenced by the environment. Thus, remarkable differences in disease transmission between the scenarios are noted. The brief stopover of the asymptomatic infector in the microenvironments leads to a peak risk of infection at 5 min (R_{\max} , the peak of infection risk). After the asymptomatic infector leaves, the quanta concentration slowly drops to a safe level (T_{terminal} , the high infection risk duration of the microenvironment). During this period, the number of all the persons who visited the microenvironment is counted (N_{\max} , the number of all exposed persons). In the case of middle- T conditions, such as case 3, case 4, and case 5 ($20\text{ }^{\circ}\text{C}$, $24\text{ }^{\circ}\text{C}$, $20\text{ }^{\circ}\text{C}$), as the RH increases gradually (30%, 60%, 80%), the R_{\max} decreases first and then increases later (3.6%, 2.1%, 4.8%); this may be because the middle RH (45–60%) is found to be the least favorable for viral survival. Furthermore, in the case of high- RH conditions such as case 1, case 5, and case 6 (90%, 80%, 95%), as the ambient T reduces gradually ($40\text{ }^{\circ}\text{C}$, $20\text{ }^{\circ}\text{C}$, and $5\text{ }^{\circ}\text{C}$), the P_v difference in vivo and in vitro gradually increases (4.27 hPa, 43.4 hPa, 53.8 hPa) and R_{\max} also shows a rising trend (2.3%, 4.8%, 5.2%). The large value for case 6 is evidently due to the low viral inactivation in the air (SARS-CoV-2 was found to survive better in low-temperature conditions) and the high deposition fraction in the respiratory tract (the supersaturated air could promote lung deposition due to the ECG effect). This could be another explanation as to why COVID-19 transmission was enhanced in the frozen seafood market, in which the environment is usually cold and damp.

The graph shows the brief stopover of the asymptomatic infector (first 5 min) and the high infection risk duration of the microenvironment (T_{terminal}). Although the quanta emission rate is consistent in each scenario, viral inactivation in the air (λ) and the deposition fraction in the respiratory tract (ω) are significantly influenced by the environment. The highest R_{\max} and the longest T_{terminal} might be an explanation as to why COVID-19 transmission was enhanced in the frozen seafood market, in which the environment is usually cold and damp (case 6).

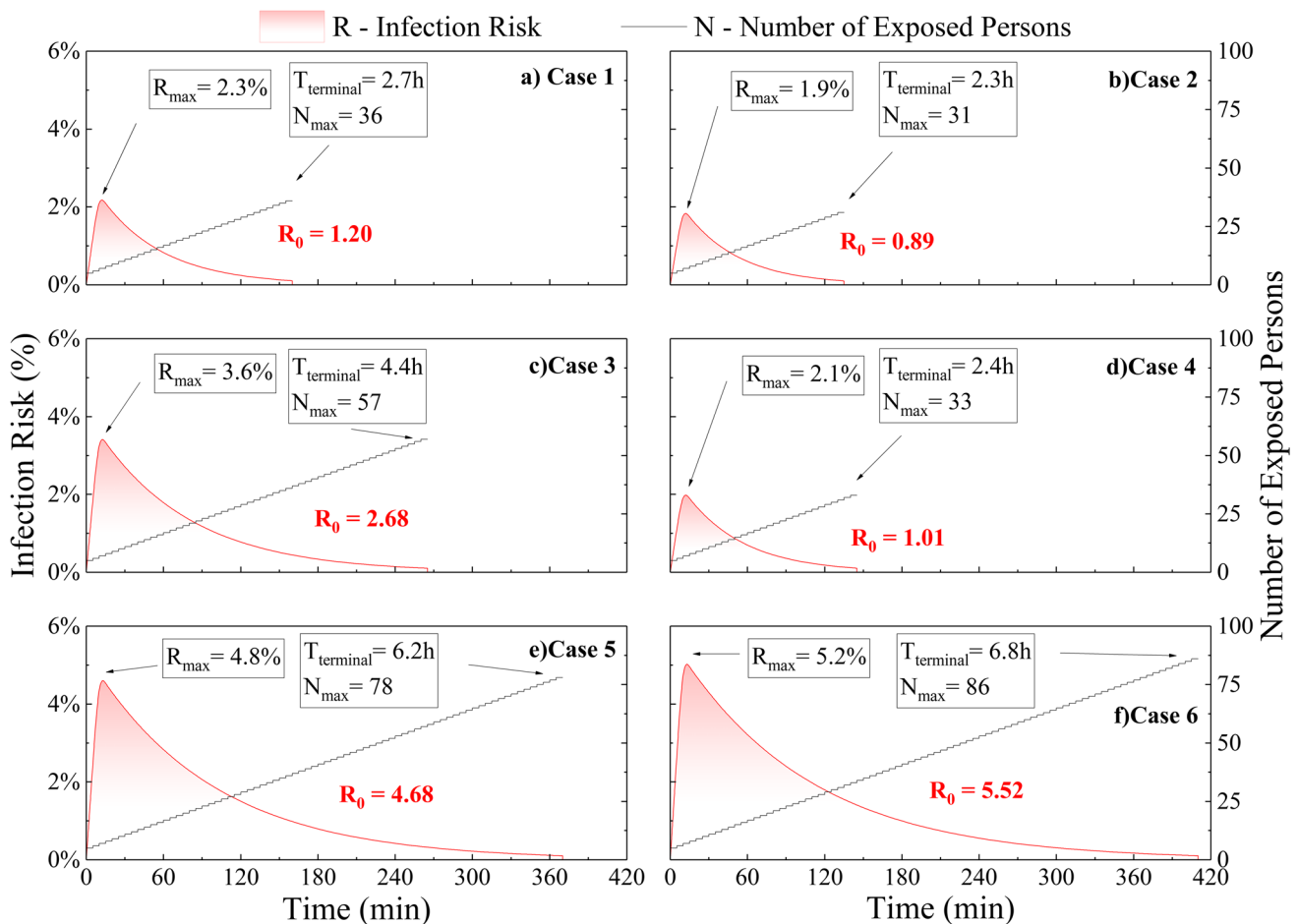


Fig. 5 Infection risk (R_{\max}) and number of the exposed persons (N_{\max}) for all scenarios

Discussion and limitations

Seasonality of COVID-19

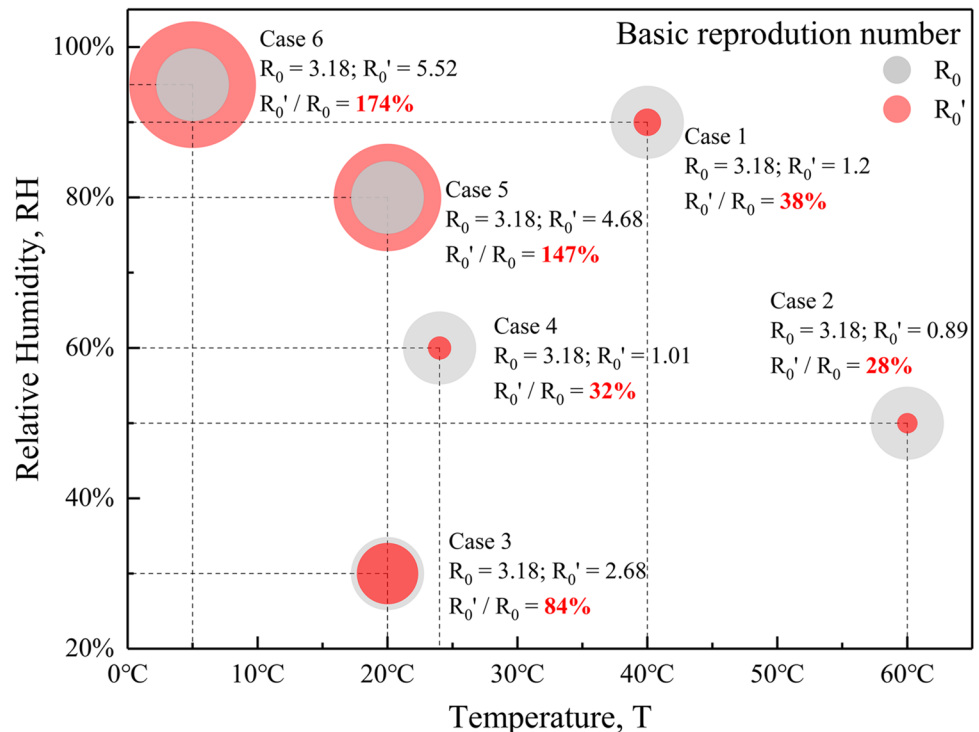
The thermal properties of ambient air, as well as relative humidity, may affect the transmissibility and viability of the virus (Rahimi et al. 2021). With the following changes in the seasons toward more temperate weather, it is of pivotal importance to know the role of environmental conditions in the transmission of the virus to raise awareness on the prevention of disease spread, and especially in a specific period (e.g., autumn, winter, spring, or summer) of a given geographical area (Coccia 2021b).

Seasonal cyclicality is a ubiquitous feature of acute respiratory infectious diseases, such as SARS and MERS (Killerby et al. 2018; Wang et al. 2020). For COVID-19, Mario Coccia (2022) found that the arithmetic mean of confirmed cases, hospitalizations of people, and admissions to intensive care units (ICUs) is significantly equal ($p < 0.01$), despite the different interventions on COVID-19 in 2020 (strong lockdowns measures) and 2021 (health policy of vaccinations).

Hence, findings here suggest that the COVID-19 pandemic is driven by seasonality and environmental factors, and the intervention strategies should be set up in summer and fully implemented during autumn and winter period (Coccia 2022b). Li et al. (2022) employed a meta-analysis to address these questions using results from 2813 published articles and observed that a rise in T would promote virus transmission in cold seasons, while significant negative influences in the warm season. RH significantly inhibited the COVID-19 transmission on the national scale. They suggested that the control measures should be developed according to local meteorological properties for the individual city (Li et al. 2022).

In this paper, we explored the complex relationship between ambient environment (T and RH) and COVID-19 transmission risk by using a modified W-R model. R_0 is the key index for evaluating the transmission risk of infectious disease (Yuan et al. 2020). Figure 6 shows the comparison between the R_0 simulated by the original W-R model and the R'_0 simulated by the modified W-R model. The original W-R model fails to consider the influence of

Fig. 6 Comparison between the R_0 simulated by the original W-R model and the R'_0 simulated by the modified W-R model



the environment on viral inactivation and droplet deposition and shows the same result for R_0 in each case, always 3.18. However, the R'_0 values simulated by the modified W-R model changed with the environmental parameters. As mentioned earlier, the middle-RH (45–60%) and high-T (>30 °C) scenarios were found to be the least favorable to the survival of the viruses (Colas et al. 2014, Harper G. 1961, Lin and Marr 2020a, Noti et al. 2013), which might be the reason why the disease infection risk is reduced in cases 1, 2, and 4. The droplet deposition risk in the airways under low-T and high-RH conditions is ignored by the original W-R model (Ishmatov 2020; Longest et al. 2011; Xi et al. 2015; Xie and Zhu 2020), which might be the reason why the disease infection risk is substantially underestimated in cases 5 and 6. In particular, the infection risk in a cold-damp scenario, such as a seafood cold store, can reach 6 times higher than in other scenarios at most.

That is, there does exist a certain range of environmental conditions that can significantly promote or inhibit the spread of COVID-19. In particular, the argument was further supported by these news that employees who worked in cold chain transportation were more vulnerable to being diagnosed with COVID-19 (<https://baijiahao.baidu.com/s?id=1728401608245389772&wfr=spider&for=pc>), and the covering of imported frozen seafood such as salmon (<http://finance.sina.com.cn/china/gncj/2020-06-13/doc-iirczymk6749091.shtml>) and shrimp (<https://www.best73.com/news/27562.html>) tested positive for SARS-CoV-2 too.

Limitations

However, several limitations of our study should be acknowledged. First, this research only focused on meteorological/weather conditions that might influence the spread of COVID-19. Further studies on the effects of artificial lockdown interventions on disease transmission, such as masks and social distance, are needed. Second, the limitations of space prevent us from covering other important meteorological factors in this study, such as air pollutant, solar radiation, and wind speed.

Xu et al. and Shen et al. found that the reduction of total aerosols in the air and the contribution of the increase in fine-mode particles during the lockdown in Wuhan (Shen et al. 2021; Xu et al. 2020b). A study from California observed that air pollutants have a significant correlation with the COVID-19 epidemic (Bashir et al. 2020). Another study also indicated that an increase in particulate matter concentration causes more COVID-19 cases and mortality (Coccia 2020a, 2021a, 2021c, 2021d; Srivastava 2021).

Despite the ultraviolet light was constantly being used for sterilization, Song et al. found that the solar radiation showed a negligibility on the COVID-19 transmission (Runkle et al. 2020), even in the comparison of high- and low-altitude regions of China (Song et al. 2022). However, a previous study reported that high solar radiation might be indicated as the main climatic factor for the tropical state that suppresses the spread of COVID-19 in Brazil (Rosario et al. 2020).

Like solar radiation, wind speed also has its two sides. Some scholars argue that the wind would accelerate the virus' travel from one location to another. This perhaps explains why the wind speed is higher, the number of cases increases in their study (Şahin 2020; Sarkodie and Owusu 2020). However, another study detected that high wind speed can be indicated as the main factor that suppresses the spread of COVID-19 (Rosario et al. 2020). Considering the transmission dynamics of the SARS-CoV-2 can also be explained by stagnation of atmospheric pollutants and viral agents, low wind speeds may promote a longer permanence of viral particles (e.g., the SARS-CoV-2) in polluted air, thus favoring the spread of COVID-19 in society (Coccia 2020c, a, 2021a, c, d, b, 2022b). Due to the highly uncertain and complex effect of environmental factors on the pandemic, the influence of meteorological factors on the newly confirmed COVID-19 cases varied greatly among existing studies, and no consistent conclusion can be drawn, which only can be controlled in laboratory experiments or model simulation (Islam et al. 2021). In order to improve the accuracy of transmission risk prediction, a more comprehensive model to analyze environment-mediated COVID-19 transmission should be employed in further research work, especially ventilation and wind speed (closely related to the HVAC system of indoor spaces). These conclusions are only a theoretical attempt since the transmission of COVID-19 is influenced by multiplicate factors.

Conclusions and prospects

The original W-R model ignored the influence of the environment on viral inactivation and droplet deposition, which might lead to the inappropriate distribution of emergency aid. In this study, a new approach is proposed to fill the gaps in knowledge when quantitatively evaluating the influence of environmental parameters on the spread of respiratory tract infections. We analyzed the currently available data on the effects of the environment on disease infection risk and identified the most critical parameters (T , RH , and P_v), and developed an alternative modified W-R model to address the aforementioned problems by proposing the dynamic virus deposition ratio (α) to assess the infection risk under varying environments. Then, it is applied to six typical exposure scenarios in daily life, reflecting how the environmental parameters are linked to viral inactivation and particle deposition, thus quantitatively affecting the transmission risk. This modified approach will enable healthcare workers and disinfection equipment to be assigned to the high-risk environment for COVID-19 prevention, before the infection outbreak, rather than passively waiting.

The results revealed that the temperature-risk relationship was negatively linear when the mean temperature was below

24 °C and became flat above 24 °C, indicating that a rise in T would significantly reduce the transmission of COVID-19 in the cold season (case 3/4/5/6), while inconspicuously negative influences in the hot season (case 1/2/4). So, the public and governments could not expect the high T to eradicate the epidemic in the hot season. The environment with middle RH has the lowest disease transmission probability. In addition, the infection risk under low- T and high- RH conditions is substantially underestimated, which should be taken seriously. In other words, high-risk environments, such as the frozen seafood market, are ill-equipped to effectively control the epidemic due to inadequate information, attention, and action, which may lead to higher risk or something even more catastrophic.

COVID-19 pandemic has threatened the public health and national security of countries seriously, which asked each country to make critical decisions to take advantage of important opportunities in the presence of highly restricted time in turbulent situations of emergency (Coccia 2020b). These measures for constraining future pandemic threats can be divided into two main categories, pharmaceutical interventions (such as vaccinations (Coccia 2022a) and health expenditures (Coccia 2021c)) and non-pharmaceutical interventions (such as lockdown policies (Askitas et al. 2021, Flaxman et al. 2020) and meteorology (Xie and Zhu 2020)). International experience of the COVID-19 pandemic crisis has shown that well-planned public policies and scientific and economic coordination policies are effective interventions for reducing high-risk aspects before and during an outbreak (Coccia 2021e, 2022c).

Recent studies show that accelerated transmission dynamics of COVID-19 is due to mainly to the mechanism of air pollution-to-human transmission (airborne viral infectivity) rather than human-to-human transmission (Coccia 2020c). The spread of COVID-19 is due to systemic causes: disease commonness (viral characteristics, transmission route), environment individuality (meteorological conditions, social context), and individual difference (disease susceptibility, immune response) (Coccia 2020c). According to a 2021 research review of the COVID-19 environment, more than 36% of them were directly or indirectly related to the indoor and outdoor environment, 16% to meteorological factors, 14% to fomites, and 34% to other factors (Rahimi et al. 2021). The still-growing body of literature on COVID-19 suggests the importance of environmental conditions in transmitting the disease beyond geographical/interpersonal borders. Despite various complicated and co-dependent factors during the COVID-19 transmission process, focusing on high-risk conditions will assist in solving these complex decision-making problems.

In general, this study suggests that sustainable science for crisis management in the presence of COVID-19 pandemic threat is also based on the cross-discipline study

of meteorology, government, and socioeconomic factors, and not only on medical research. The high-risk condition may generate most part of the infections and indicate that selected containment measures are more sustainable social policy than a blind full lockdown, which provides useful information for policymakers if the COVID-19 coexists with humans for a long time.

Supplementary Information The online version contains supplementary material available at <https://doi.org/10.1007/s11356-022-21766-x>.

Data availability All data used during the study are available from the corresponding author by request.

Author contribution Ning Mao: data curation, writing – original draft preparation

Dingkun Zhang: reviewing and editing

Yupei Li: reviewing and editing

Ying Li: reviewing and editing

Jin Li: reviewing

Li Zhao: reviewing

Qingqin Wang: reviewing

Zhu Cheng: supervision

Yin Zhang: supervision

Enshen Long: conceptualization, methodology, supervision

Funding This work was supported by the National Natural Science Foundation of China (52078314).

Declarations

Ethics approval and consent to participate Not applicable.

Consent for publication Not applicable.

Competing interests The authors declare no competing interests.

References

- Adams WC (1993) Measurement of breathing rate and volume in routinely performed daily activities. final report, Human Performance Lab, California University
- Ahmadi M, Sharifi A, Dorosti S, Jafarzadeh Ghouschi S, Ghanbari N (2020) Investigation of effective climatology parameters on COVID-19 outbreak in Iran. *Sci Total Environ* 729:138705. <https://doi.org/10.1016/j.scitotenv.2020.138705>
- Akhbarizadeh R, Dobaradaran S, Torkmahalle A (2021): Suspended fine particulate matter (PM_{2.5}), microplastics (MPs), and polycyclic aromatic hydrocarbons (PAHs) in air: their possible relationships and health implications. *Environ Res* <https://doi.org/10.1016/j.envres.2020.110339>
- Alfano FRA, Dell'Isola M, Ficco G, Tassini F (2012) Experimental analysis of air tightness in Mediterranean buildings using the fan pressurization method. *Build Environ* 53:16–25. <https://doi.org/10.1016/j.buildenv.2011.12.017>
- Asgari M, Lucci F, Kuczaj AK (2019) Multispecies aerosol evolution and deposition in a bent pipe. *J Aerosol Sci* 129:53–70. <https://doi.org/10.1016/j.jaerosci.2018.12.007>
- Askitas N, Tatsiramos K, Verheyden B (2021) Estimating worldwide effects of non-pharmaceutical interventions on COVID-19 incidence and population mobility patterns using a multiple-event study. *Sci Rep* 11:1972. <https://doi.org/10.1038/s41598-021-81442-x>
- Austin E, Brock J, Wissler E (2010) A model for deposition of stable and unstable aerosols in the human respiratory tract. *Am Ind Hyg Assoc J*. <https://doi.org/10.1080/15298667991430703>
- Azman AS, Luquero FJ (2020) From China: hope and lessons for COVID-19 control. *Lancet Infect Dis* 20:756–757. [https://doi.org/10.1016/S1473-3099\(20\)30264-4](https://doi.org/10.1016/S1473-3099(20)30264-4)
- Bashir MF, Ma BJ, Bilal KB, Bashir MA, Farooq TH, Iqbal N, Bashir M (2020) Correlation between environmental pollution indicators and COVID-19 pandemic: a brief study in Californian context. *Environ Res* 187:109652. <https://doi.org/10.1016/j.envres.2020.109652>
- Bin S-C, Zang S-Z, Jing-Ru G, Jian-Fa W, Li-Ping Z (2018) HMGB1-mediated differential response on hippocampal neurotransmitter disorder and neuroinflammation in adolescent male and female mice following cold exposure. *Brain Behav Immun*. <https://doi.org/10.1016/j.bbi.2018.11.313>
- Borro L, Mazzei L, Raponi M, Piscitelli P, Miani A, Secinaro A (2020) The role of air conditioning in the diffusion of Sars-CoV-2 in indoor environments: a first computational fluid dynamic model, based on investigations performed at the Vatican State Children's hospital. *Environ Res* 110343. <https://doi.org/10.1016/j.envres.2020.110343>
- Briz-Redón Á, Serrano-Aroca Á (2020) A spatio-temporal analysis for exploring the effect of temperature on COVID-19 early evolution in Spain. *Sci Total Environ* 728:138811. <https://doi.org/10.1016/j.scitotenv.2020.138811>
- Buonanno G, Stabile L, Morawska L (2020) Estimation of airborne viral emission: quanta emission rate of SARS-CoV-2 for infection risk assessment. *Environ Int* 141:105794. <https://doi.org/10.1016/j.envint.2020.105794>
- Chatoutsidou SE, Lazaridis M (2019) Assessment of the impact of particulate dry deposition on soiling of indoor cultural heritage objects found in churches and museums/libraries. *J Cult Herit* 39:221–228. <https://doi.org/10.1016/j.culher.2019.02.017>
- China (1998) Public bathhouse Health Standard(GB/ T17220-1998). State Bureau of Technical Supervision of China, pp. 4 (in Chinese)
- China (2010) Code for design of cold storage(GB50072-2010). Ministry of housing and urban rural development of China, pp. 135p:A4 (in Chinese)
- China (2017) Requirements and evaluation methods of indoor human thermal comfort environment(GB/T 33658-2017). National Standardization Administration Committee, pp. 24 (in Chinese)
- Coccia M (2020a) How (Un)sustainable environments are related to the diffusion of COVID-19: the relation between coronavirus disease 2019, air pollution, wind resource and energy. *Sustainability* 12. <https://doi.org/10.3390/su12229709>
- Coccia M (2020b) Comparative critical decisions in management. *Global Encyclopedia of Public Administration, Public Policy, and Governance*, 1-10, https://doi.org/10.1007/978-3-319-31816-5_3969-1
- Coccia M (2020c) Factors determining the diffusion of COVID-19 and suggested strategy to prevent future accelerated viral infectivity similar to COVID. *Sci Total Environ* 729:138474. <https://doi.org/10.1016/j.scitotenv.2020.138474>
- Coccia M (2021a) The effects of atmospheric stability with low wind speed and of air pollution on the accelerated transmission dynamics of COVID-19. *Int J Environ Stud* 78:1–27. <https://doi.org/10.1080/00207233.2020.1802937>
- Coccia M (2021b) The impact of first and second wave of the COVID-19 pandemic in society: comparative analysis to support control measures to cope with negative effects of future

- infectious diseases. *Environ Res* 197:111099. <https://doi.org/10.1016/j.envres.2021.111099>
- Coccia M (2021c) High health expenditures and low exposure of population to air pollution as critical factors that can reduce fatality rate in COVID-19 pandemic crisis: a global analysis. *Environ Res* 199:111339. <https://doi.org/10.1016/j.envres.2021.111339>
- Coccia M (2021d) How do low wind speeds and high levels of air pollution support the spread of COVID-19? *Atmos Pollut Res* 12:437–445. <https://doi.org/10.1016/j.apr.2020.10.002>
- Coccia M (2021e) Pandemic prevention: lessons from COVID-19. *Encyclopedia* 1:433–444. <https://doi.org/10.3390/encyclopedia1020036>
- Coccia M (2022a) Optimal levels of vaccination to reduce COVID-19 infected individuals and deaths: a global analysis. *Environ Res* 204. <https://doi.org/10.1016/j.envres.2021.112314>
- Coccia M (2022b) COVID-19 pandemic over 2020 (with lockdowns) and 2021 (with vaccinations): similar effects for seasonality and environmental factors. *Environ Res* 208:112711. <https://doi.org/10.1016/j.envres.2022.112711>
- Coccia M (2022c) Preparedness of countries to face COVID-19 pandemic crisis: strategic positioning and factors supporting effective strategies of prevention of pandemic threats. *Environ Res* 203:111678. <https://doi.org/10.1016/j.envres.2021.111678>
- Colas A, Estienney M, Aho S, Perrier-Cornet JM, de Rougemont A, Pothier P, Gervais P, Belliot G (2014) Absolute humidity influences the seasonal persistence and infectivity of human norovirus. *Appl Environ Microbiol* 80:7196–7205. <https://doi.org/10.1128/AEM.01871-14>
- Deng L, Ma P, Wu Y, Ma Y, Yang X, Li Y, Deng Q (2020) High and low temperatures aggravate airway inflammation of asthma: evidence in a mouse model. *Environ Pollut* 256:113433. <https://doi.org/10.1016/j.envpol.2019.113433>
- Diao Y, Kodera S, Anzai D, Gomez-Tames J, Rashed EA, Hirata A (2021) Influence of population density, temperature, and absolute humidity on spread and decay durations of COVID-19: a comparative study of scenarios in China, England, Germany, and Japan. *One Health* 12:100203. <https://doi.org/10.1016/j.onehlt.2020.100203>
- Doremalen NV, Bushmaker T, Munster V (2013) Stability of Middle East respiratory syndrome coronavirus (MERS-CoV) under different environmental conditions. *Eurosurveillance* 18. <https://doi.org/10.2807/1560-7917.ES2013.18.38.20590>
- Fierce L, Robey AJ, Hamilton C (2021) Simulating near-field enhancement in transmission of airborne viruses with a quadrature-based model. *Indoor Air* 31:1843–1859. <https://doi.org/10.1111/ina.12900>
- Flaxman S, Mishra S, Gandy A, Unwin HJT, Mellan TA, Coupland H, Whittaker C, Zhu H, Berah T, Eaton JW, Monod M, Imperial College C-RT, Ghani AC, Donnelly CA, Riley S, Vollmer MAC, Ferguson NM, Okell LC, Bhatt S (2020) Estimating the effects of non-pharmaceutical interventions on COVID-19 in Europe. *Nature* 584:257–261. <https://doi.org/10.1038/s41586-020-2405-7>
- Fröhlich-Nowoisky J, Kampf CJ, Weber B, Huffman JA, Pöhlker C, Andreae MO, Lang-Yona N, Burrows SM, Gunthe SS, Elbert W, Su H, Hoor P, Thines E, Hoffmann T, Després VR, Pöschl U (2016) Bioaerosols in the Earth system: climate, health, and ecosystem interactions. *Atmos Res* 182:346–376. <https://doi.org/10.1016/j.atmosres.2016.07.018>
- Gammaitoni L, Nucci MC (1997) Using a mathematical model to evaluate the efficacy of TB control measures. *Emerg Infect Dis* 3:335–342. <https://doi.org/10.3201/eid0303.970310>
- Gba B, Ls A, Lm BJEI (2020) Estimation of airborne viral emission: quanta emission rate of SARS-CoV-2 for infection risk assessment - ScienceDirect. *Environ Int* 141. <https://doi.org/10.1016/j.envint.2020.105794>
- Grallton J, Tovey E, McLaws ML, Rawlinson WD (2011) The role of particle size in aerosolised pathogen transmission: a review. *J Inf Secur* 62:1–13. <https://doi.org/10.1016/j.jinf.2010.11.010>
- Guo Y, Qian H, Sun Z, Cao J, Liu F, Luo X, Ling R, Weschler LB, Mo J, Zhang Y (2021) Assessing and controlling infection risk with Wells-Riley model and spatial flow impact factor (SFIF). *Sustain Cities Soc* 67:102719. <https://doi.org/10.1016/j.scs.2021.102719>
- Haque SE, Rahman M (2020) Association between temperature, humidity, and COVID-19 outbreaks in Bangladesh. *Environ Sci Pol* 114:253–255. <https://doi.org/10.1016/j.envsci.2020.08.012>
- Harper GJ (1961) Airborne micro-organisms: survival tests with four viruses. *J Hyg* 59:479. <https://doi.org/10.1017/s0022172400039176>
- Harrichandra A, Ierardi AM, Pavilonis B (2020) An estimation of airborne SARS-CoV-2 infection transmission risk in New York City nail salons. *Toxicol Ind Health* 36:074823372096465. <https://doi.org/10.1177/0748233720964650>
- ICRP (1994) Summary description of respiratory tract dosimetry model. *Ann ICRP* 24:106–120. [https://doi.org/10.1016/0146-6453\(94\)90038-8](https://doi.org/10.1016/0146-6453(94)90038-8)
- Ishmatov A (2020) Influence of weather and seasonal variations in temperature and humidity on supersaturation and enhanced deposition of submicron aerosols in the human respiratory tract. *Atmos Environ* 223. <https://doi.org/10.1016/j.atmosenv.2019.117226>
- Islam N, Bukhari Q, Jameel Y, Shabnam S, Erzurumluoglu AM, Siddique MA, Massaro JM, D'Agostino RB (2021) COVID-19 and climatic factors: a global analysis. *Environ Res* 193. <https://doi.org/10.1016/j.envres.2020.110355>
- Keene CH (1955) Airborne contagion and air hygiene. *William Firth Wells* 25:249–249. <https://doi.org/10.1111/j.1746-1561.1955.tb08015.x>
- Killerby ME, Biggs HM, Haynes A, Dahl RM, Mustaqim D, Gerber SI, Watson JT (2018) Human coronavirus circulation in the United States 2014–2017. *J Clin Virol* 101:52–56. <https://doi.org/10.1016/j.jcv.2018.01.019>
- Kim JW, Xi J, Si XA (2013) Dynamic growth and deposition of hygroscopic aerosols in the nasal airway of a 5-year-old child. *Int J Numer Meth Bio* 29:17–39. <https://doi.org/10.1002/cnm.2490>
- Knight V (2010) Viruses as agents of airborne contagion. *Ann N Y Acad Sci* 353:147–156. <https://doi.org/10.1111/j.1749-6632.1980.tb18917.x>
- Kreyling GAFHG (1984) Conditions for measuring supersaturation in the human lung using aerosols. *J Aerosol Sci*. [https://doi.org/10.1016/0021-8502\(84\)90065-X](https://doi.org/10.1016/0021-8502(84)90065-X)
- Lai CC, Shih TP, Ko WC, Tang HJ, Hsueh PR (2020) Severe acute respiratory syndrome coronavirus 2 (SARS-CoV-2) and coronavirus disease-2019 (COVID-19): the epidemic and the challenges. *Int J Antimicrob Agents* 55:105924. <https://doi.org/10.1016/j.ijantimicag.2020.105924>
- Li H-L, Yang B-Y, Wang L-J, Liao K, Sun N, Liu Y-C, Ma R-F, Yang X-D (2022) A meta-analysis result: uneven influences of season, geo-spatial scale and latitude on relationship between meteorological factors and the COVID-19 transmission. *Environ Res* 212:113297. <https://doi.org/10.1016/j.envres.2022.113297>
- Li Y, Duan S, Yu ITS, Wong TWJ (2010) Multi-zone modeling of probable SARS virus transmission by airflow between flats in Block E, Amoy Gardens. *Indoor Air* 15:96–111. <https://doi.org/10.1111/j.1600-0668.2004.00318.x>
- Lin C, Lau AKH, Fung JCH, Guo C, Chan JWM, Yeung DW, Zhang Y, Bo Y, Hossain MS, Zeng Y, Lao XQ (2020) A mechanism-based parameterisation scheme to investigate the association between transmission rate of COVID-19 and meteorological factors on plains in China. *Sci Total Environ* 737:140348. <https://doi.org/10.1016/j.scitotenv.2020.140348>
- Lin K, Marr LC (2020a) Humidity-dependent decay of viruses, but not bacteria, in aerosols and droplets follows disinfection kinetics.

- Environ Sci Technol 54:1024–1032. <https://doi.org/10.1021/acs.est.9b04959>
- Lin K, Marr LC (2020b) Humidity-dependent decay of viruses, but not bacteria, in aerosols and droplets follows disinfection kinetics. *Environ Sci Technol* 54:1024–1032. <https://doi.org/10.1021/acs.est.9b04959>
- Liu J, Zhou J, Yao J, Zhang X, Li L, Xu X, He X, Wang B, Fu S, Niu T, Yan J, Shi Y, Ren X, Niu J, Zhu W, Li S, Luo B, Zhang K (2020a) Impact of meteorological factors on the COVID-19 transmission: a multi-city study in China. *Sci Total Environ* 726:138513. <https://doi.org/10.1016/j.scitotenv.2020.138513>
- Liu Y, Ning Z, Chen Y, Guo M, Liu Y, Gali NK, Sun L, Duan Y, Cai J, Westerdahl D, Liu X, Ho K-f, Kan H, Fu Q, Lan K (2020b) Aerodynamic characteristics and RNA concentration of SARS-CoV-2 aerosol in Wuhan hospitals during COVID-19 outbreak. *BioRxiv* <https://doi.org/10.1101/2020.03.08.982637>
- Longest PW, Hindle M (2010) CFD simulations of enhanced condensational growth (ECG) applied to respiratory drug delivery with comparisons to in vitro data. *J Aerosol Sci* 41:805–820. <https://doi.org/10.1016/j.jaerosci.2010.04.006>
- Longest PW, Hindle M (2011) Numerical model to characterize the size increase of combination drug and hygroscopic excipient nanoparticle aerosols. *Aerosol Sci Technol* 45:884–899. <https://doi.org/10.1080/02786826.2011.566592>
- Longest PW, Tian G, Hindle M (2011) Improving the lung delivery of nasally administered aerosols during noninvasive ventilation—an application of enhanced condensational growth (ECG). *J Aerosol Med Pulm D* 24:103–118. <https://doi.org/10.1089/jamp.2010.0849>
- Ma Y, Zhao Y, Liu J, He X, Wang B, Fu S, Yan J, Niu J, Zhou J, Luo B (2020) Effects of temperature variation and humidity on the death of COVID-19 in Wuhan, China. *Sci Total Environ* 724:138226. <https://doi.org/10.1016/j.scitotenv.2020.138226>
- Mao N, An CK, Guo LY, Wang M, Guo L, Guo SR, Long ES (2020) Transmission risk of infectious droplets in physical spreading process at different times: a review. *Build Environ* 185. <https://doi.org/10.1016/j.buildenv.2020.107307>
- Marmett B, Pires Dorneles G, Boek Carvalho R, Peres A, Roosevelt Torres Romao P, Barcos Nunes R, Ramos Rhoden C (2020) Air pollution concentration and period of the day modulates inhalation of PM_{2.5} during moderate- and high-intensity interval exercise. *Environ Res* 110528. <https://doi.org/10.1016/j.envres.2020.110528>
- Mendez-Arriaga F (2020) The temperature and regional climate effects on communitarian COVID-19 contagion in Mexico throughout phase I. *Sci Total Environ* 735:139560. <https://doi.org/10.1016/j.scitotenv.2020.139560>
- Menebo MM (2020) Temperature and precipitation associate with Covid-19 new daily cases: a correlation study between weather and Covid-19 pandemic in Oslo, Norway. *Sci Total Environ* 737:139659. <https://doi.org/10.1016/j.scitotenv.2020.139659>
- Morawska L et al (2020) How can airborne transmission of COVID-19 indoors be minimised? *Environ Int* 142. <https://doi.org/10.1016/j.envint.2020.105832>
- Morrow PE (2010) Physics of airborne particles and their deposition in the lung. *Ann N Y Acad Sci* 353:71–80. <https://doi.org/10.1111/j.1749-6632.1980.tb18908.x>
- Nan ZH, Li Z, Yang SS, Jun T, Hong CZ (2009) Seasonal characteristics of clinical rate of influenza-like illness in Shenzhen and its meteorological forecast model. *Meteorol Sci Technol* 37:709–712. <https://doi.org/10.3969/j.issn.1671-6345.2009.06.014> (in Chinese)
- Nicas M, Hubbard WVN, Alan (2005) Toward understanding the risk of secondary airborne infection: emission of respirable pathogens. *J Occup Environ Hyg*. <https://doi.org/10.1080/15459620590918466>
- Nordsiek F, Bodenschatz E, Bagheri G (2021) Risk assessment for airborne disease transmission by poly-pathogen aerosols. *PLoS One* 16:e0248004. <https://doi.org/10.1371/journal.pone.0248004>
- Noti JD, Blachere FM, McMillen CM, Lindsley WG, Kashon ML, Slaughter DR, Beezhold DH (2013) High humidity leads to loss of infectious influenza virus from simulated coughs. *PLoS One* 8:e57485. <https://doi.org/10.1371/journal.pone.0057485>
- Pani SK, Lin N-H, RavindraBabu S (2020) Association of COVID-19 pandemic with meteorological parameters over Singapore. *Sci Total Environ* 740. <https://doi.org/10.1016/j.scitotenv.2020.140112>
- Pica N, Bouvier NMJCOiV (2012) Environmental factors affecting the transmission of respiratory viruses. 2, 90-95. <https://doi.org/10.1016/j.coviro.2011.12.003>
- Prata DN, Rodrigues W, Bermejo PH (2020) Temperature significantly changes COVID-19 transmission in (sub)tropical cities of Brazil. *Sci Total Environ* 729:138862. <https://doi.org/10.1016/j.scitotenv.2020.138862>
- Pu X, Wang L, Chen L, Pan J, Tang L, Wen J, Qiu H (2020) Differential effects of size-specific particulate matter on lower respiratory infections in children: a multi-city time-series analysis in Sichuan, China. *Environ Res* 193:110581. <https://doi.org/10.1016/j.envres.2020.110581>
- Pyankov OV, Bodnev SA, Pyankova OG, Agranovski IE (2018) Survival of aerosolized coronavirus in the ambient air. *J Aerosol Sci* 115:158–163. <https://doi.org/10.1016/j.jaerosci.2017.09.009>
- Qian H, Zheng XH, Zhang XJ (2012): Prediction model of air borne infection probability of respiratory infectious diseases *Journal of Southeast University (Natural Science Edition)* 42, 468-472 10.3969/j.issn.1001—0505.2012.03.014 (in Chinese)
- Rahimi NR, Fouladi-Fard R, Aali R, Shahryari A, Rezaali M, Ghafouri Y, Ghalhari MR, Asadi-Ghalhari M, Farzinnia B, Conti Gea O, Fiore M (2021) Bidirectional association between COVID-19 and the environment: a systematic review. *Environ Res* 194. <https://doi.org/10.1016/j.envres.2020.110692>
- Riley EC, Murphy G, Riley RL (1978) Airborne spread of measles in a suburban elementary school. *Am J Epidemiol* 421-32. <https://doi.org/10.1093/ajep/107.3.269>
- Rosario DKA, Mutz YS, Bernardes PC, Conte-Junior CA (2020) Relationship between COVID-19 and weather: case study in a tropical country. *Int J Hyg Environ Health* 229:113587. <https://doi.org/10.1016/j.ijheh.2020.113587>
- Rothman KJ, Greenland S, Lash TL (2011) *Modern epidemiology: third edition*, 1-758 pp
- Runkle JD, Sugg MM, Leeper RD, Rao Y, Matthews JL, Rennie JJ (2020) Short-term effects of specific humidity and temperature on COVID-19 morbidity in select US cities. *Sci Total Environ* 740:140093. <https://doi.org/10.1016/j.scitotenv.2020.140093>
- Şahin M (2020) Impact of weather on COVID-19 pandemic in Turkey. *Sci Total Environ* 728:138810. <https://doi.org/10.1016/j.scitotenv.2020.138810>
- Sarangapani R, Wexler AS (1996) Growth and neutralization of sulfate aerosols in human airways. *J Aerosol Sci* 81:480–490. <https://doi.org/10.1055/s-2007-972910>
- Sarkodie SA, Owusu PA (2020) Impact of meteorological factors on COVID-19 pandemic: evidence from top 20 countries with confirmed cases. *Environ Res* 191:110101. <https://doi.org/10.1016/j.envres.2020.110101>
- Sattar S, Ijaz MK, Johnson-Lussenburg C, Springthorpe V (1984) Effect of relative humidity on the airborne survival of rotavirus SAI. <https://doi.org/10.1128/AEM.47.4.879-881.1984>
- Sharma R, Balasubramanian R (2020) Evaluation of the effectiveness of a portable air cleaner in mitigating indoor human exposure to cooking-derived airborne particles. *Environ Res* 183. <https://doi.org/10.1016/j.envres.2020.109192>

- Shen L, Zhao T, Wang H, Liu J, Bai Y, Kong S, Zheng H, Zhu Y, Shu Z (2021) Importance of meteorology in air pollution events during the city lockdown for COVID-19 in Hubei Province, Central China. *Sci Total Environ* 754:142227. <https://doi.org/10.1016/j.scitotenv.2020.142227>
- Sobral MFF, Duarte GB, da Penha Sobral AIG, Marinho MLM, de Souza MA (2020) Association between climate variables and global transmission of SARS-CoV-2. *Sci Total Environ* 729:138997. <https://doi.org/10.1016/j.scitotenv.2020.138997>
- Song P, Han H, Feng H, Hui Y, Zhou T, Meng W, Yan J, Li J, Fang Y, Liu P, Li X, Li X (2022) High altitude Relieves transmission risks of COVID-19 through meteorological and environmental factors: evidence from China. *Environ Res* 212:113214. <https://doi.org/10.1016/j.envres.2022.113214>
- Srivastava A (2021) COVID-19 and air pollution and meteorology—an intricate relationship: a review. *Chemosphere* 263:128297. <https://doi.org/10.1016/j.chemosphere.2020.128297>
- Stabile L, Dell'Isola M, Russi A, Massimo A, Buonanno G (2017) The effect of natural ventilation strategy on indoor air quality in schools. *Sci Total Environ* 595:894–902. <https://doi.org/10.1016/j.scitotenv.2017.03.048>
- Tian G, Longest PW, Su G, Hindle M (2011) Characterization of respiratory drug delivery with enhanced condensational growth using an individual path model of the entire tracheobronchial airways. *Ann Biomed Eng* 39:1136–1153. <https://doi.org/10.1007/s10439-010-0223-z>
- Tosepu R, Gunawan J, Effendy DS, Ahmad LOAI, Lestari H, Bahar H, Asfian P (2020) Correlation between weather and Covid-19 pandemic in Jakarta, Indonesia. *Sci Total Environ* 725:138436. <https://doi.org/10.1016/j.scitotenv.2020.138436>
- Urrego J, Ko AI, da Silva Santos Carbone A, Paiao DS, Sgarbi RV, Yeckel CW, Andrews JR, Croda J (2015) The impact of ventilation and early diagnosis on tuberculosis transmission in Brazilian prisons. *Am J Trop Med Hyg* 93:739–746. <https://doi.org/10.4269/ajtmh.15-0166>
- van Doremalen N, Bushmaker T, Morris DH, Holbrook MG, Gamble A, Williamson BN, Tamin A, Harcourt JL, Thornburg NJ, Gerber SI, Lloyd-Smith JO, de Wit E, Munster VJ (2020) Aerosol and surface stability of SARS-CoV-2 as compared with SARS-CoV-1. *New Engl J Med* 382:1564–1567. <https://doi.org/10.1056/NEJMc2004973>
- Vuorinen V et al (2020) Modelling aerosol transport and virus exposure with numerical simulations in relation to SARS-CoV-2 transmission by inhalation indoors. *Saf Sci* 130:104866. <https://doi.org/10.1016/j.ssci.2020.104866>
- Wagner BG, Coburn BJ, Blower S (2009) Calculating the potential for within-flight transmission of influenza A (H1N1). *BMC Med* 7:81. <https://doi.org/10.1186/1741-7015-7-81>
- Walsh KA, Jordan K, Clyne B, Rohde D, Drummond L, Byrne P, Ahern S, Carty PG, O'Brien KK, O'Murchu E, O'Neill M, Smith SM, Ryan M, Harrington P (2020) SARS-CoV-2 detection, viral load and infectivity over the course of an infection. *J Inf Secur* 81:357–371. <https://doi.org/10.1016/j.jinf.2020.06.067>
- Wang J, Tang K, Feng K, Lin X, Lv W, Chen K, Wang F (2020) High temperature and high humidity reduce the transmission of COVID-19. *Soc Sci Electron Pub*. <https://doi.org/10.2139/ssrn.3551767>
- Watanabe T, Bartrand TA, Weir MH, Omura T, Haas CN (2010) Development of a dose-response model for SARS coronavirus. *Risk Anal* 30:1129–1138. <https://doi.org/10.1111/j.1539-6924.2010.01427.x>
- Wei J, Li YJAAJoIC (2016) Airborne spread of infectious agents in the indoor environment. 44, S102-S108. <https://doi.org/10.1016/j.ajic.2016.06.003>
- Winkler-Heil R, Pichelstorfer L, Hofmann W (2017) Aerosol dynamics model for the simulation of hygroscopic growth and deposition of inhaled NaCl particles in the human respiratory tract. *J Aerosol Sci* 113:212–226. <https://doi.org/10.1016/j.jaerosci.2017.08.005>
- Wu Y, Jing W, Liu J, Ma Q, Yuan J, Wang Y, Du M, Liu M (2020) Effects of temperature and humidity on the daily new cases and new deaths of COVID-19 in 166 countries. *Sci Total Environ* 729:139051. <https://doi.org/10.1016/j.scitotenv.2020.139051>
- Xi J, Kim J, Si XA, Zhou Y (2013) Hygroscopic aerosol deposition in the human upper respiratory tract under various thermo-humidity conditions. *J Environ Sci Health A Tox Hazard Subst Environ Eng* 48:1790–1805. <https://doi.org/10.1080/10934529.2013.823333>
- Xi J, Si XA, Kim JW (2015) Chapter 5. Characterizing respiratory airflow and aerosol condensational growth in children and adults using an imaging-CFD approach. Elsevier Inc, 125-155. <https://doi.org/10.1016/b978-0-12-408077-5.00005-5>
- Xie J, Zhu Y (2020) Association between ambient temperature and COVID-19 infection in 122 cities from China. *Sci Total Environ* 724. <https://doi.org/10.1016/j.scitotenv.2020.138201>
- Xu H, Yan C, Fu Q, Xiao K, Yu Y, Han D, Wang W, Cheng J (2020a) Possible environmental effects on the spread of COVID-19 in China. *Sci Total Environ* 731:139211. <https://doi.org/10.1016/j.scitotenv.2020.139211>
- Xu K, Cui K, Young L-H, Hsieh Y-K, Wang Y-F, Zhang J, Wan S (2020b) Impact of the COVID-19 event on air quality in Central China. *Aerosol Air Qual Res* 20:915–929. <https://doi.org/10.4209/aaqr.2020.04.0150>
- Yan C (2015) Experimental study on indoor thermal environment of residential buildings in North China in winter. *Shanxi Architecture* 41, 198-199 (in Chinese), CNKI:SUN:JZSX.0.2015-35-109
- Yeh HC, Raabe RFP (1976) Factors influencing the deposition of inhaled particles. *Environ Health Perspect* 15:147–156. <https://doi.org/10.2307/3428398>
- Yu ITS, Li Y, Wong TW, Tam W, Chan AT, Lee J, W H (2004) Evidence of airborne transmission of the severe acute respiratory syndrome virus. *New Engl J Med* 17:1731–1739. <https://doi.org/10.1056/NEJMoa032867>
- Yuan J, Li M, Lv G, Lu ZK (2020) Monitoring transmissibility and mortality of COVID-19 in Europe. *Int J Infect Dis* 95:311–315. <https://doi.org/10.1016/j.ijid.2020.03.050>
- Zhai Z, Li H (2021) Distributed probability of infection risk of airborne respiratory diseases. *Indoor Built Environ*. <https://doi.org/10.1177/1420326x211030324>
- Zhang X, Ji Z, Yue Y, Liu H, Wang J (2020) Infection Risk Assessment of COVID-19 through Aerosol Transmission: a case study of south China seafood market. *Environ Sci Technol*. <https://doi.org/10.1021/acs.est.0c02895>
- Zhou J, Koutsopoulos HN (2021) Virus transmission risk in urban rail systems: microscopic simulation-based analysis of spatio-temporal characteristics. *Transport Res Record J Transport Res Board* 2675:120–132 (in Chinese). <https://doi.org/10.1177/03611981211010181>

Publisher's note Springer Nature remains neutral with regard to jurisdictional claims in published maps and institutional affiliations.